Supporting Online Material for

A competitive inhibitor traps LeuT in an open-to-out conformation

Satinder K. Singh, Chayne L. Piscitelli, Atsuko Yamashita, and Eric Gouaux

This PDF file includes:

EXPERIMENTAL PROCEDURES

Protein Expression and Purification for Functional Experiments

LeuT protein reconstituted into lipid vesicles was expressed and purified as described previously (*S1*). Protein employed for both the radioligand binding and fluorescence titration experiments was purified similarly (*S2*) except for the presence of 100 mM L-alanine during the solubilization and NiNTA chromatographic steps to displace the endogenously-bound L-leucine. The alanine concentration was subsequently decreased to 20 mM during the size-exclusion chromatographic (SEC) step in buffer I (20 mM HEPES-Tris [pH 7.0], 100 mM choline chloride) containing 1 mM n-dodecyl-β-D-maltoside [DDM] and then finally allowed to fall below 100 nM during extensive dialysis against the same buffer. All functional data were analyzed via nonlinear regression in GraphPad Prism 4.03.

Preparation of LeuT Proteoliposomes

LeuT was reconstituted into lipid vesicles with a 1:110 protein:lipid ratio and loaded with buffer II (20 mM HEPES-Tris [pH 7.0], 100 mM potassium gluconate) as outlined elsewhere (*S2*).

Inhibition of Binding and Transport Screens

These experiments were performed at 20ºC as described (*S2*). For binding, a typical reaction contained 100 nM LeuT, 50 nM L-[^{3}H]leucine (11.7 Ci/mmol), and 1 mM of the indicated amino acid (none for the positive control), along with 1 mM DDM, in buffer III (20 mM HEPES-Tris [pH 7.0], 100 mM NaCl). Nonspecific binding obtained in the presence of 1 mM alanine was subtracted from each data point, and binding was terminated as described (*S2*). For transport, a typical reaction contained 0.5

μg protein diluted 200-fold into buffer III containing 50 nM [^{3}H]leucine (117 Ci/mmol). Nonspecific uptake into liposomes devoid of protein and subjected to the same experimental conditions was subtracted from the corresponding LeuT data points to determine specific uptake, and transport was terminated as described (*S2*). For both binding and transport screens, the entire experiment was performed twice, each time in triplicate, and the data normalized to that measured in the absence of competing amino acid.

Saturation Binding

Binding was initiated by adding LeuT to a final concentration of 20 nM in 500 μl buffer III containing 1 mM DDM and 0.5-200 nM [^{3}H]leucine (23.4 Ci/mmol), 10-4000 nM [^{3}H]alanine (14.3 Ci/mmol), or 2-500 nM L-[^{3}H]methionine (41 Ci/mmol). Reactions were rotated at room temperature for 2 hours and then terminated as described (*S2*) except that the filters for [^{3}H]alanine and [^{3}H]methionine were washed only once or twice, respectively. Nonspecific binding obtained in the presence of 1 mM alanine was subtracted from each data point. Experiments were performed at least three times, each time in duplicate, and the data were fit to a single-site rectangular hyperbola.

Competition Binding

Binding inhibition assays were performed by equilibrating 20 nM solubilized LeuT in buffer III with 1 mM DDM and 20 nM [^{3}H]leucine (58.5 Ci/mmol) up to 15 hours at room temperature with competing cold L-amino acids at the following concentration ranges: 0-10 μM leucine, 0-100 μM methionine, 0-1 mM tyrosine, 0-1 mM L-4-F-Phe, 0-500 mM glycine, 0-10 mM alanine, and 0-10 mM tryptophan. Reactions were terminated, and the filters were washed as outlined (*S2*). The experiments were

performed at least twice, each time in duplicate, and the data were normalized to that measured in the absence of competing amino acid and fit to a sigmoidal dose response equation. IC_{50}s were converted to K_is with the Cheng-Prusoff equation (*S3*) using a leucine dissociation constant of 17 nM.

Steady-State Kinetics

Transport was initiated at 20°C by diluting LeuT proteoliposomes (0.05 μg per assay for [^{3}H]leucine, [^{3}H]alanine, and [^{3}H]methionine or 0.5 μg per assay for [^{3}H]glycine and L-[^{3}H]tyrosine) 200-fold into buffer III containing varying concentrations of one of the five amino acids mentioned above: 0.5-800 nM [^{3}H]leucine (117 Ci/mmol), 25-5000 nM [^{3}H]alanine (17.9 Ci/mmol), 15-1600 nM [^{3}H]methionine (41 Ci/mmol), 100-30000 nM [^{3}H]glycine (14 Ci/mmol), or 100-20000 nM [^{3}H]tyrosine (20 Ci/mmol). For the lowest and highest concentrations of each amino acid, preliminary experiments established that flux remained linear for up to 10 min. Reactions were terminated after six minutes essentially as outlined (*S2*), and each experiment was performed at least twice in triplicate, with data being fit to the Michaelis-Menten equation.

Tryptophan Time Course

LeuT-proteoliposomes (1.3 μg/mL in buffer III) were incubated at 20^{o}C with 1 uM [^{3}H]tryptophan (31 Ci/mmol) for up to 90 minutes. At the indicated time points, 200 μL-aliquots of the reaction mix was removed and quenched as described previously (*S2*) For the positive control, LeuT-proteoliposomes were similarly incubated with 100 nM [^{3}H]alanine, with 200-ul aliquots removed at intervening time points up to 12 minutes. Non-specific flux was measured by repeating the time course using liposomes devoid of

protein. The experiment was conducted twice in duplicate, and data were fit to a single exponential.

Binding versus Transport Time Course

These experiments were performed as outlined for the tryptophan time course with two exceptions. First, the reaction buffer contained 70 nM [^{3}H]leucine (117 Ci/mmol), 290 nM [^{3}H]alanine (71.7 Ci/mmol), 145 nM [^{3}H]methionine (81 Ci/mmol), 955 nM [^{3}H]glycine (56 Ci/mmol), or 1415 nM [^{3}H]tyrosine (40 Ci/mmol), concentrations which are ~ 50% of the respective Michaelis constants. Second, two sets of LeuT liposomes were prepared, one loaded with buffer III to measure transport, the other loaded with buffer II to measure binding. The assay was performed twice, each time in duplicate, and the data were fit to a single exponential.

Inhibition Kinetics

These experiments were conducted as delineated for [^{3}H]alanine steady-state kinetics except that a concentration range of 50-8000 nM [^{3}H]alanine (14.3 Ci/mmol) was used in the presence of three different tryptophan concentrations (0, 2, and 50 μM), and the assays were performed in the dark to minimize photooxidation of tryptophan (*S4*). The experiment was replicated once, each time in triplicate, and the data were fit to the Michaelis-Menten equation.

Preparation of LeuT-amino acid Complex Crystals

The LeuT-Ala complex was prepared as described (*S2*). LeuT-Met was prepared similarly except for the substitution of 10 mM methionine and 1 mM dithiothreitol (DTT) for alanine during the size exclusion chromatographic (SEC) and dialysis steps. LeuT-Leu and LeuT-SeMet were also prepared similarly except for the substitution during the

SEC step of 30 mM leucine for the LeuT-Leu complex and 30 mM selenomethionine and 1 mM DTT for the LeuT-SeMet complex. LeuT-Gly was prepared with buffer containing 50 mM tryptophan during the solubilization step, 10 mM tryptophan during the NiNTA chromatographic step, and 200 mM glycine during the SEC step. LeuT-4-L-F-Phe was prepared similarly except that the pooled NiNTA fractions were applied to a series of two PD10 columns pre-equilibrated with buffer containing 20 mM TrisHCl (pH 7.0), 190 mM NaCl, 10 mM KCl, 1 mM DDM, and 8 mM D,L-4-F-Phe. Final dialysis subsequent to SEC was then performed against buffer containing 40 mM β-OG and 40 mM L-4-F-Phe. The presence of L-4-F-Phe in all samples was facilitated by monitoring a distinct, sharp absorbance peak at 262 nm that was easily distinguishable from the protein absorbance peak at 280 nm.

LeuT-Trp was prepared with the presence of 50 mM tryptophan in all buffers, and protein concentration was monitored with the Bradford assay. Some of the LeuT-Trp protein was applied to an analytical SEC column (Superose 6) to exchange the 40 mM n-octyl-β-D-glucopyranoside (β-OG) with 30 mM seleno-heptylglucoside. This would permit unambiguous placement of detergent molecules in the resulting crystal structures (see below). Selenomethionine-labeled protein (SeMet-LeuT) was expressed in C41 cells essentially as described (*S5*) and purified as outlined for LeuT-Trp except for the addition of 1 mM β-mercaptoethanol (βME) in all buffers.

LeuT protein was concentrated to 3-6 mg/ml and subjected to crystallization trials via hanging drop vapor diffusion. Crystals for the most of the "occluded state" structures grew within 7-10 days at 20°C in the presence of 17-22% PEG 550 MME, 100 mM HEPES-NaOH (pH 7-7.5), and 200 mM NaCl. The best-diffracting crystals for the more

"open" LeuT-Trp structure also grew under similar conditions except in the presence of 400 mM NaCl and in the dark. The best-diffracting crystals for the LeuT-Gly and –L-4-F-Phe complexes grew within a similar time frame and temperature except in the presence of 24-26% PEG 550 MME and 400 mM NaCl.

Structure Determination

Native diffraction data were collected at 110K at NSLS beam line X29A or ALS beam line 8.2.2 at an X-ray wavelength of 1.0000 Å with the exception of data for LeuT-Ala, -Met, and -Trp crystals, which were collected at 1.1000 Å, 1.7712 Å, and 0.9796 Å, respectively. Diffraction data for all selenium-containing crystal complexes were collected at 0.9796 Å in 45° wedges (inverse beam strategy). All datasets were processed using HKL2000 (*S6*). Selenium sites were located with SOLVE (*S7*) and confirmed with strong peaks (>5σ) in anomalous difference Fourier maps.

Phases for the LeuT-Gly, -Ala, Leu (30 mM), -Met, -SeMet, and –L-4-F-Phe, complexes were obtained via molecular replacement with MOLREP (*S8*) or AMORE (*S9*) using the LeuT-Leu structure (PDB ID 2A65) devoid of water, leucine, and sodium as the starting model. Initial phases for the LeuT-Trp complex were also calculated by molecular replacement (MOLREP) (*S10*) using a modified version of 2A65 in which portions of TM1, TM6, EL4a, and EL4b had been deleted. These phases were significantly improved by rigid-body refinement in REFMAC (*S11*) and simulated annealing in CNS (*S12*). As independent verification of these phases, experimental phases obtained from a single-wavelength anomalous dispersion (SAD) experiment (*S13*) on a selenomethionine-substituted LeuT-Trp cocrystal were calculated, and the SeMet-LeuT-Trp structure solved (data not shown). Refinement for all structures proceeded

with iterative rounds of manual rebuilding in O (*S14*) and COOT (*S15*) with the assistance of sigmaA-weighted 2*F*o-*F*c and *F*o-*F*c maps as well as simulated-annealing *F*o-*F*c omit maps followed by maximum-likelihood based energy minimization and isotropic B-factor refinement in CNS (*S12*) or REFMAC5 (*S10*). Ramachandran geometry is excellent for all structures, with greater than 93% of the residues in the most favored regions and none in disallowed regions. For each data set, 5% of the reflections were removed for cross-validation.

Conformational Shift Analysis

The conformational shifts observed between the LeuT-Trp and LeuT-Leu (PDB ID 2A65) complexes were analyzed (PDB ID 2A65) with DynDom (*S16*). The moving domain elements were manually assigned by first superposing the two structures using all Cα atoms in residue ranges 5-22, 55-203, 257-287, and 322-511 (RMSD = 0.41 Å). The definitions of the moving elements were subsequently modified by superposing the intervening regions of the structures and observing the RMSD fit. Two elements were identified that, when fit independently as rigid bodies, largely define the differences between the two structures. One element is composed of residues 23-54 and 241-257, which superposes with a Cα RMSD of 0.35 Å. The second element is composed of residues 304-320, which superposes with a Cα RMSD of 1.39 Å. These "moving domain" definitions were independently input into DynDom via web server access (http://fizz.cmp.uea.ac.uk/dyndom/) to calculate the degree of rotation and location of the axes.

Movie S1. Structural conformational changes depicted for isomerization of LeuT between the substrate-bound occluded and the competitive inhibitor-bound open-to-out states. The beginning and end states are the crystal structures of the LeuT-Leu and LeuT-Trp complexes, respectively. The structure is viewed parallel to the membrane plane, initially with all helices shown. In the second part, portions of TM10 and TM11 have been removed (residues 407-419 and 450-477) for clarity and residues that comprise part of the extracellular gate (R30, D404, Y108, and F253) are shown as sticks. Coloring is the same as that in Fig. 3C of the main text. Intermediate states were calculated by linear interpolation between the two sets of crystallographic coordinates as implemented by the CNS morphing script from the Yale Morph Server (http://molmovdb.org) (*S17, S18*).

References

S1. A. Yamashita, S. K. Singh, T. Kawate, Y. Jin, E. Gouaux, *Nature* **437**, 215 (2005).
S2. S. K. Singh, A. Yamashita, E. Gouaux, *Nature* **448**, 952 (2007).
S3. Y. Cheng, W. H. Prusoff, *Biochem. Pharmacol.* **22**, 3099 (1973).
S4. R. S. Asquith, D. E. Rivett, *Biochim. Biophys. Acta* **252**, 111 (1971).
S5. G. D. Van Duyne, R. F. Standaert, P. A. Karplus, S. L. Schreiber, J. Clardy, *J. Mol. Biol.* **229**, 105 (1993).
S6. Z. Otwinowski, W. Minor, *Methods in Enzymol.* **276**, 307 (1997).
S7. T. C. Terwilliger, J. Berendzen, *Acta Crystallogr. D Biol. Crystallogr.* **55**, 849 (1999).
S8. A. Vagin, A. Teplyakov, *Acta Crystallogr. D Biol. Crystallogr.* **56**, 1622 (2000).
S9. J. Navaza, *Acta Crystallogr.* **A50**, 157 (1994).
S10. *Acta Crystallogr. D Biol. Crystallogr.* **50**, 760 (1994).
S11. G. N. Murshudov, A. A. Vagin, E. J. Dodson, *Acta Crystallogr. D Biol. Crystallogr.* **53**, 240 (1997).
S12. A. T. Brunger *et al.*, *Acta Crystallogr. D Biol. Crystallogr.* **54**, 905 (1998).
S13. W. A. Hendrickson, *Science* **254**, 51 (1991).
S14. T. A. Jones, J. Y. Zou, S. W. Cowan, Kjeldgaard, *Acta Crystallogr. A* **47 (Pt 2)**, 110 (1991).
S15. P. Emsley, K. Cowtan, *Acta Crystallogr. D Biol. Crystallogr.* **60**, 2126 (2004).
S16. S. Hayward, R. A. Lee, *J. Mol. Graph. Model* **21**, 181 (2002).
S17. N. Echols, D. Milburn, M. Gerstein, *Nucleic Acids Res.* **31**, 478 (2003).

S18. W. G. Krebs, M. Gerstein, *Nucleic Acids Res.* **28**, 1665 (2000).

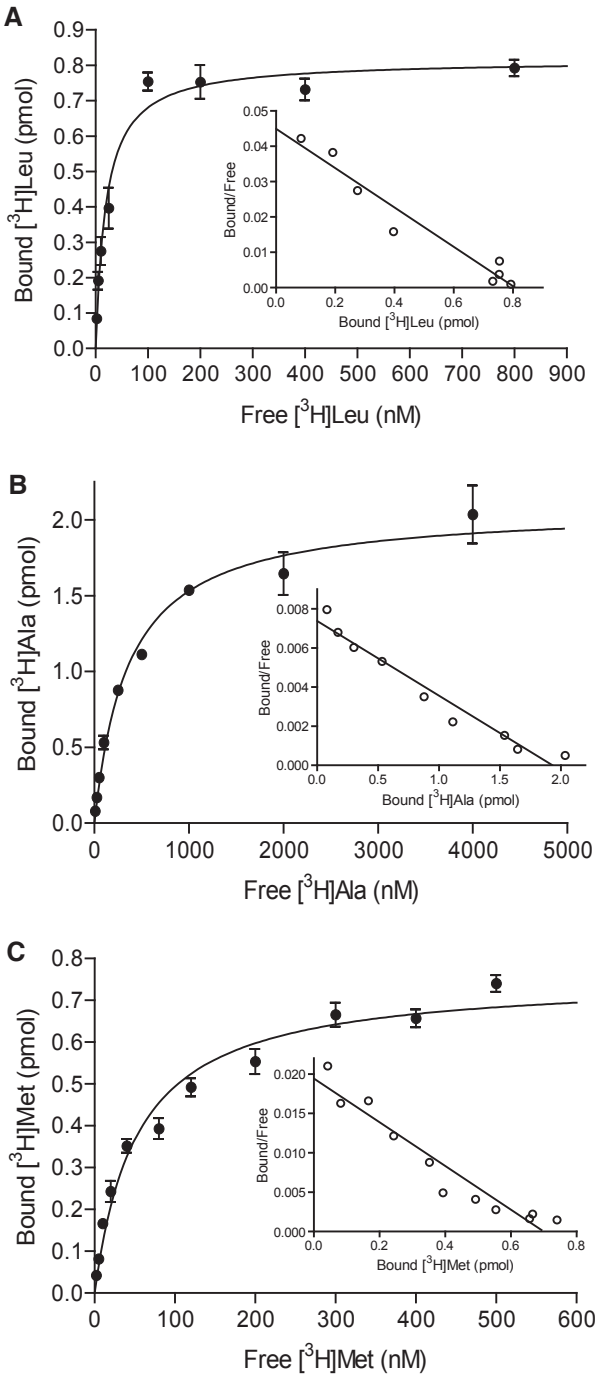

Fig. S1. Radioligand binding data. Saturation binding plots for (**A**) [^{3}H]leucine, (**B**) [^{3}H]alanine, and (**C**) [^{3}H]methionine with Scatchard insets. Data are shown as mean +/- SEM (vertical bars, $N = 2$).

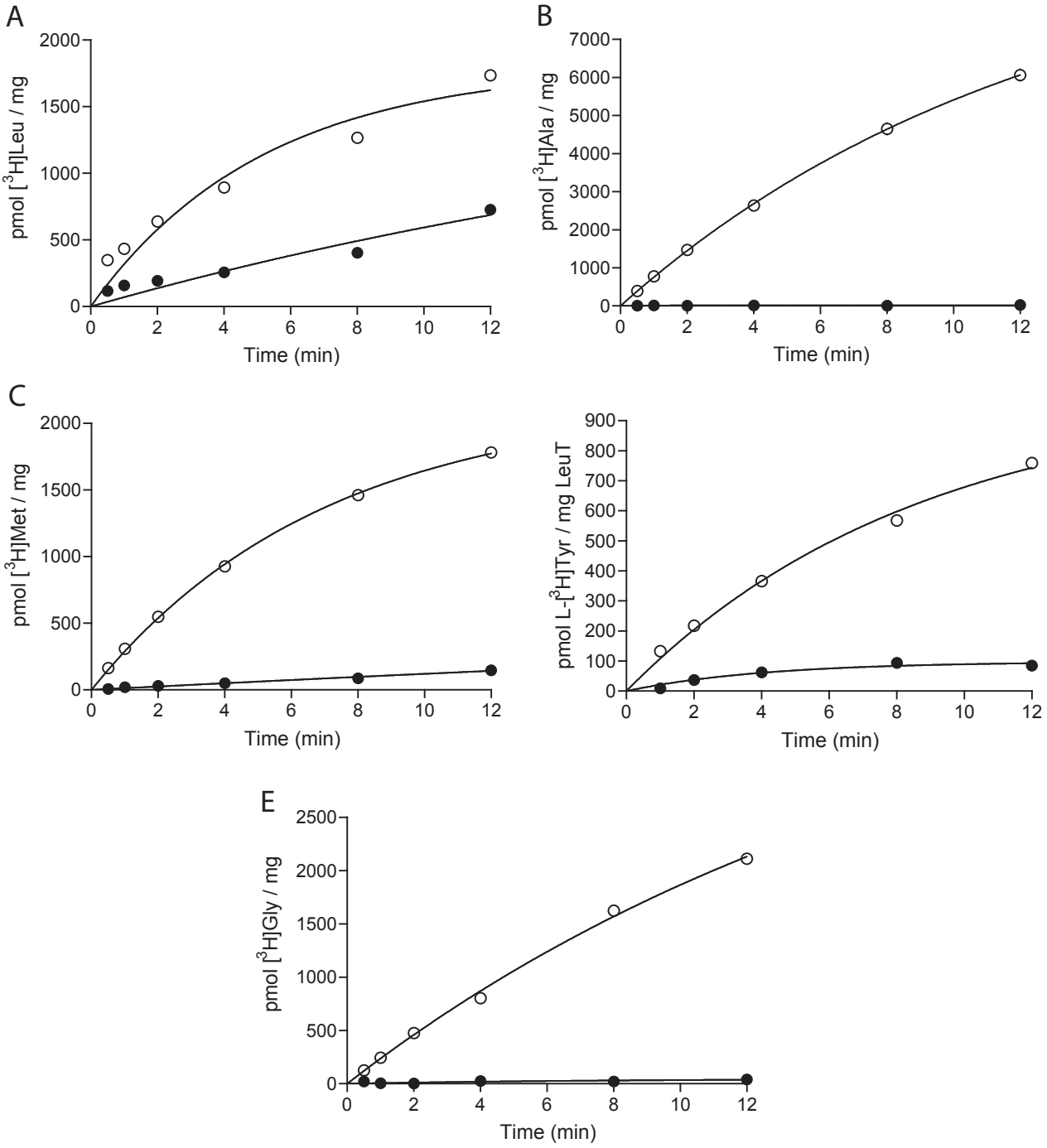

Fig. S2. Transport versus binding control experiments for the five amino acid substrates examined. Transport by (open circles) and binding to (filled circles) for (A) [^{3}H]leucine, (B) [^{3}H]alanine, (C) [^{3}H]methionine, (D) [^{3}H]tyrosine, and (E) [^{3}H]glycine. Data shown are mean values (N = 2).

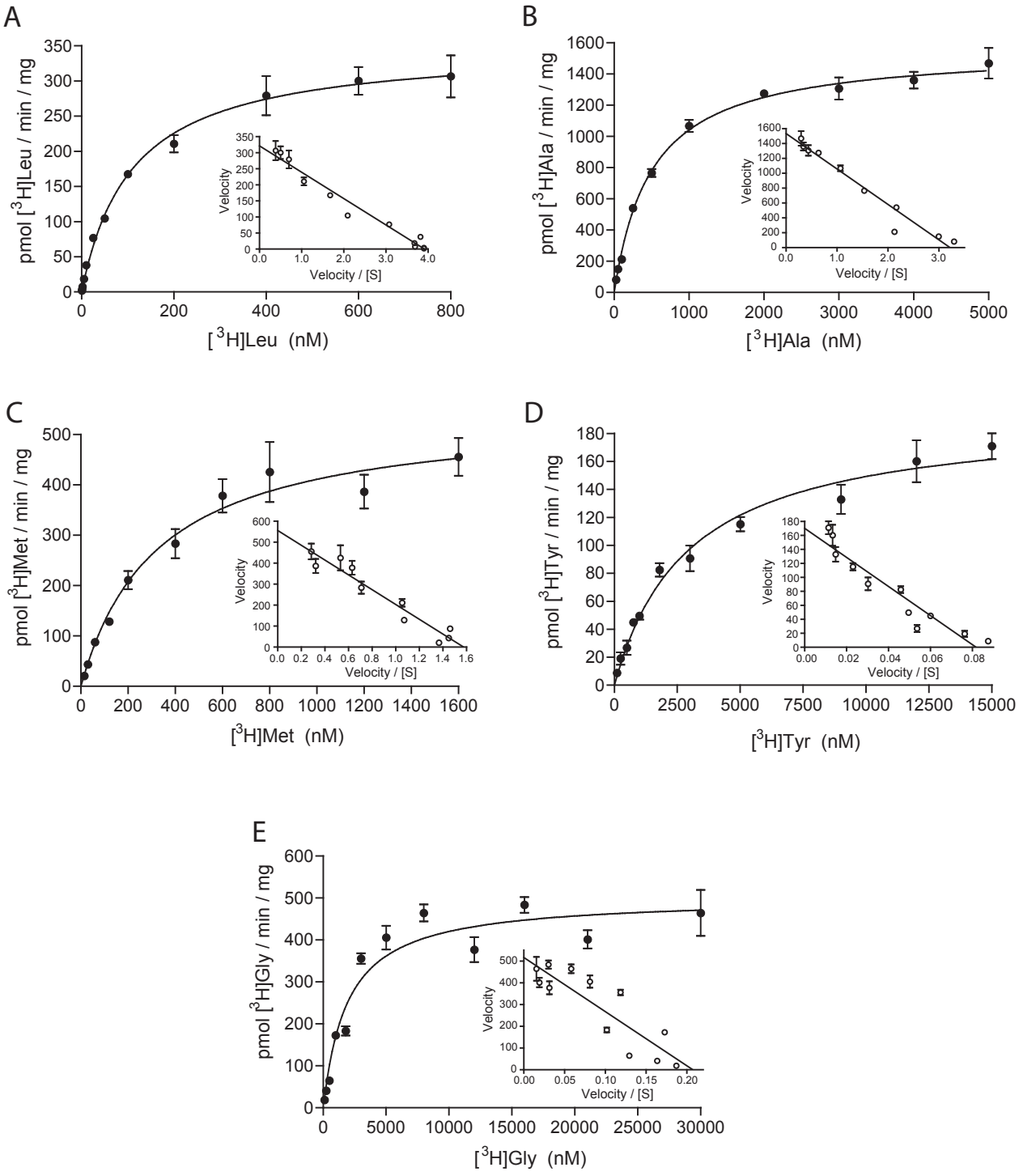

Fig. S3. Steady-state kinetics. Michaelis-Menten plots for (A) [^{3}H]leucine, (B) [^{3}H]alanine, (C) [^{3}H]methionine, (D) [^{3}H]tyrosine, and (E) [^{3}H]glycine with Eadie-Hofstee insets. Data shown are mean +/- SEM (vertical bars, N = 3).

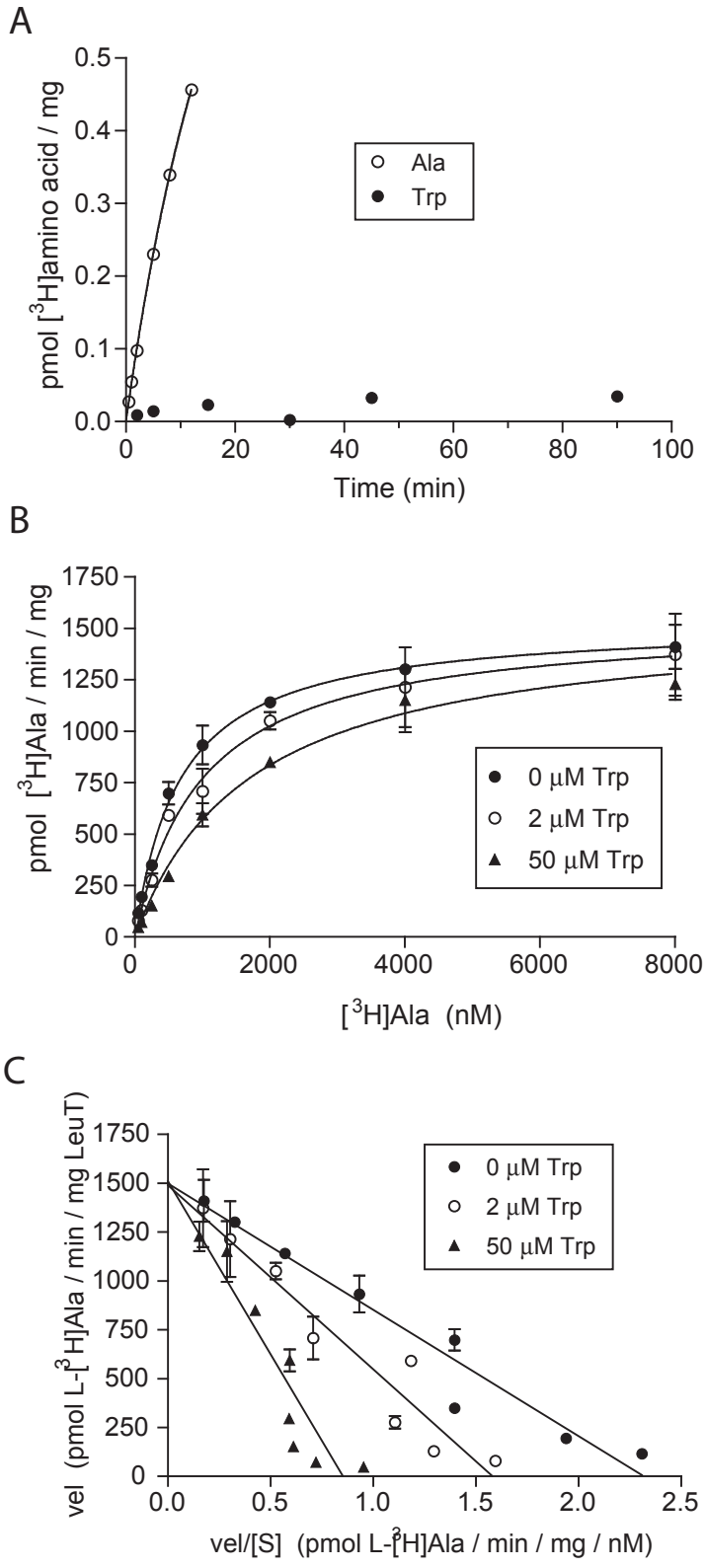

Fig. S4. L-tryptophan is a nontransportable, competitive inhibitor of LeuT. (A) Time course of 100 nM [^{3}H]alanine (open circles) versus 1 μM [^{3}H]tryptophan transport demonstrating that tryptophan is not a substrate. (B) Steady-state kinetics (Michaelis-Menten plot) of inhibition of [^{3}H]alanine transport by 1, 2, and 50 μM tryptophan. (C) Eadie-Hofstee plot of the same data shown in (B). Data are shown as mean values in A (N = 2) or mean +/- SEM (vertical bars, N = 3) in B and C.

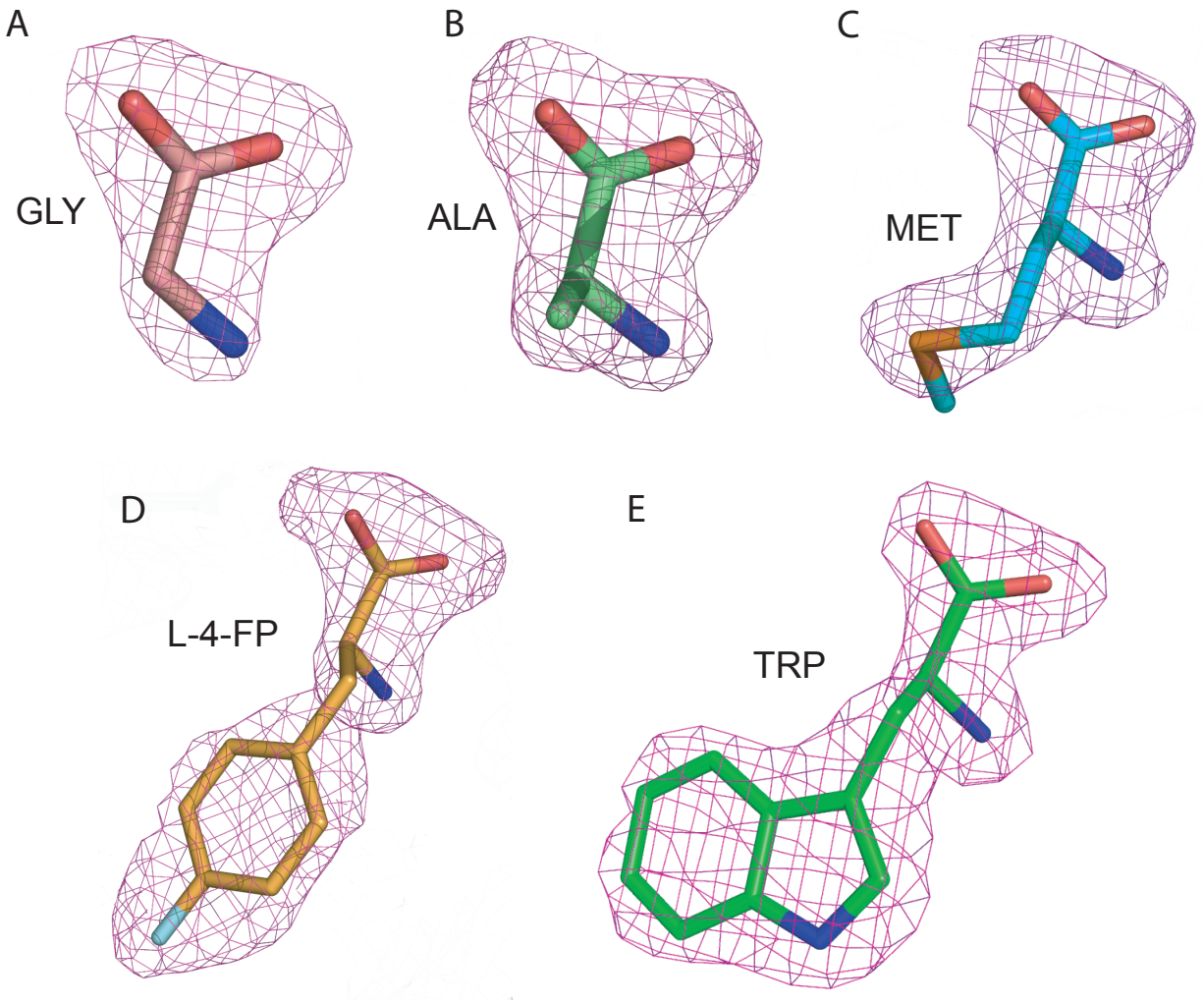

Fig. S5. Simulated-annealing omit electron density maps (contoured at 3σ) of amino acids bound in the substrate binding pocket of LeuT (the "601" site). (A) Glycine, (B) alanine, (C) methionine, (D) L-4-fluorophenylalanine, and (E) tryptophan. In each case, the respective amino acid was omitted from the simulated annealing run and subsequent phase calculation.

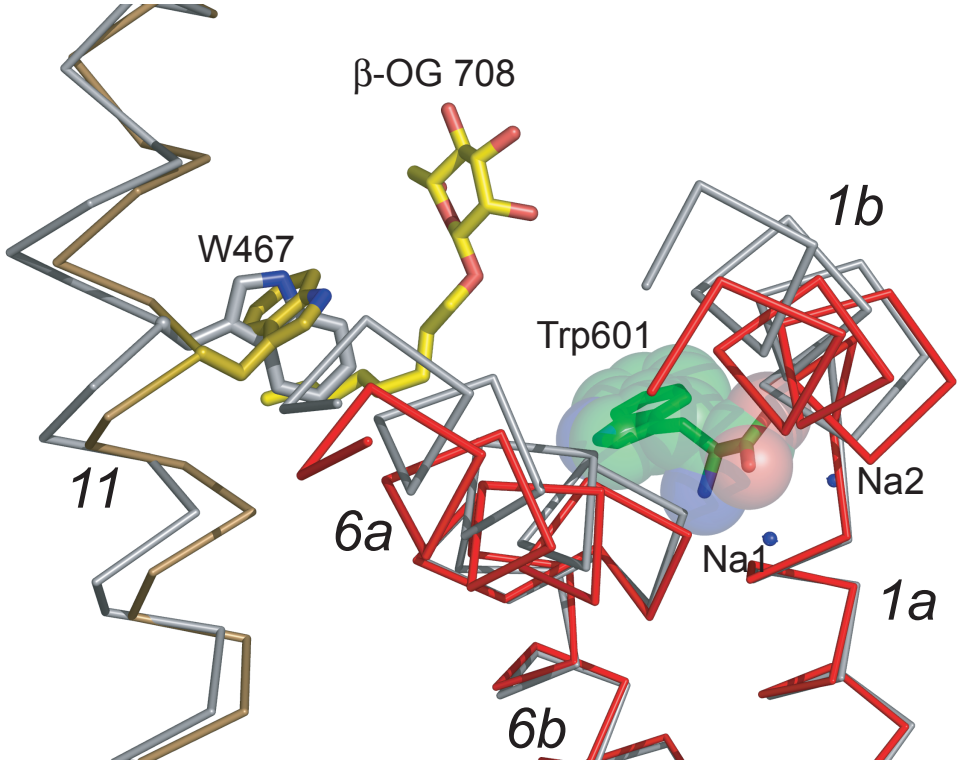

Fig. S6. Overlay of the LeuT-Trp and -Leu complexes at TM11. Cα traces of TMs1b, 6a, and 11 for the LeuT-Trp (sand and red) and -Leu (gray) complexes. W467 from each structure is also depicted in the same colors. The carbon and oxygen atoms of β-OG 708 from the LeuT-Trp structure are colored yellow and red, respectively.

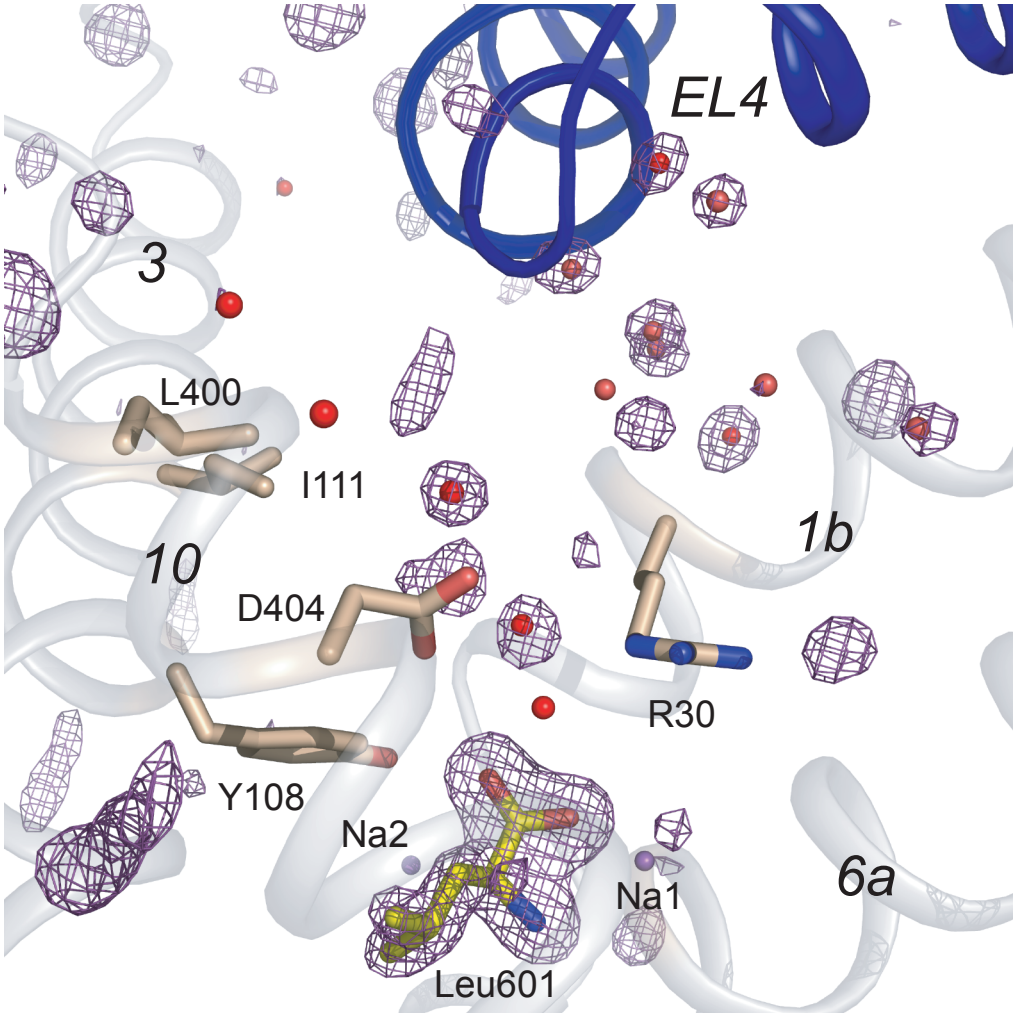

Fig. S7. View of the LeuT-Leu complex (crystallized in the presence of 30 mM leucine). The extracellular vestibule is shown, along with EL4 (blue), TMs 1b, 3, 6a, and 10 (transparent gray), and residues R30, Y108, I111, L400, and D404. Also depicted are Leu601 (yellow) and water molecules (red spheres) in the vestibule. Simulated annealing F_o-F_c omit map, contoured at 4σ, in which Leu601 and solvent molecules were omitted from the F_c calculation. There is clear density for leucine in the primary substrate binding pocket but not in the vestibule.

Table S1: LeuT/Substrate/Inhibitor Data Collection Statistics

	Glycine	**Alanine**	**Leucine**[a]	**Methionine**	**SelenoMet**	**L-4-F-Phe**[b]	**Tryptophan**
Beamline	ALS 8.2.2	NSLS X29A	ALS 8.2.2	ALS 8.2.2	ALS 8.2.2	ALS 8.2.2	ALS 8.2.2
Wavelength (Å)	1.0000	1.1000	1.0000	1.7712	0.9794	1.0000	0.9796
Space Group	C2	C2	C2	C2	C2	C2	C2
Cell Dimensions							
a, b, c (Å)	90.1, 86.6, 81.5	89.4, 87.2, 81.2	89.4, 86.7, 81.4	88.3, 86.6, 81.2	89.8, 86.7, 81.7	90.1, 86.3, 81.6	88.6, 85.2, 82.3
α, β, γ (º)	90.0, 95.3, 90.0	90.0, 95.9, 90.0	90.0, 95.9, 90.0	90.0, 95.6, 90.0	90.0, 95.9, 90.0	90.0, 95.2, 90.0	90.0, 93.3, 90.0
Resolution (Å)	50.00-2.15	50.00 - 1.90	80.85-1.80	47.51-2.30	81.38-1.95	62.3-2.10	50.00-2.00
R_{merge} (%)[c, d]	7.7 (76.3)	6.3 (52.2)	5.0 (75.0)	8.0 (32.1)	7.0 (76.8)	7.8 (52.7)	8.4 (73.4)
$I/\sigma I$ [c]	30.0 (1.9)	39.2 (2.4)	34.7 (2.7)	22.2 (1.6)	28.0 (2.6)	15.9 (1.7)	11.1 (1.1)
Completeness (%)[c]	98.6 (90.3)	99.9 (99.9)	99.0 (98.1)	87.7 (53.4)	99.5 (98.2)	92.3 (64.3)	97.4 (90.4)
Redundancy[c]	6.7 (5.4)	4.6 (2.8)	7.3 (6.8)	6.3 (2.5)	7.4 (6.7)	3.5 (2.6)	2.6 (2.3)

[a] Structure determined in the presence of 30 mM Leu.

[b] Abbreviation for the tyrosine analogue, L-4-fluorophenylalanine.

[c] Number in parentheses represents statistics for data in the highest resolution shell, 2.23-2.15 Å, 1.97-1.90 Å, 1.86-1.80 Å, 2.38-2.30 Å, 2.02-1.95 Å, 2.18-2.10 Å, and 2.07-2.00 Å for the LeuT-Gly, -Ala, -Leu, -Met, -SeMet, -L-4-F-Phe, and -Trp, data sets, respectively.

[d] $R_{merge} = \sum_{hkl}\sum_i |I_i(hkl)_i - \langle I(hkl)\rangle| / \sum_{hkl}\sum_i I_i(hkl)$.

Table S2: LeuT/Substrate/Inhibitor Refinement Statistics

	Glycine	**Alanine**	**Leucine**[a]	**Methionine**	**SelenoMet**	**L-4-F-Phe**[b]	**Tryptophan**
Resolution (Å)	50.00-2.15	50.00 - 1.90	50.00-1.80	50.0-2.30	50.00-1.95	62.30-2.10	50.00-2.00
No. reflections	33,833	48,834	57,474	26,640	45,397	31,935	41,152
R_{work}[c]/R_{free}[d] (%)	19.6/22.8	21.1/22.9	18.0/20.5	19.7/22.4	19.2/21.8	19.6/23.7	19.8 /23.0
No. atoms	4190	4298	4343	4211	4116	4280	4327
Protein [e]	4045	4074	4045	4045	4268	4077	4010
Substrate/Inhibitor	10	6	9	9	9	13	60
Na^+	2	2	2	2	2	2	2
β-OG	60	120	134	100	60	100	160
Water	73	96	153	55	112	88	95
B-factors (Å^2)							
Overall	50.6	41.3	37.5	47.2	39.4	40.2	42.0
Protein	49.6	40.1	36.2	47.4	39.0	39.4	38.1
Substrate/Inhibitor	38.0	26.6	22.1	38.6	26.8	29.6	26.8
Inhibitor 2	n/a [f]	n/a [f]	n/a [f]	n/a [f]	n/a [f]	n/a [f]	55.7 [g]
Na^+	38.0	27.1	22.6	33.6	24.9	27.6	11.9
β-OG	87.5	79.5	67.7	86.2	55.4	74.8	67.2
Water	53.5	47.3	46.3	50.7	46.3	40.6	39.3
RMSD [h]							
Bond lengths (Å)	0.006	0.006	0.011	0.007	0.003	0.006	0.008
Bond angles (º)	0.889	1.095	1.244	0.970	0.729	0.989	1.050
Ramachandran Plot [i]	93.6, 6.2, 0.2, 0.0	94.1, 5.7, 0.2, 0.0	94.7, 5.3, 0.0, 0.0	95.0, 5.0, 0.0, 0.0	94.5, 5.5, 0.0, 0.0	94.7, 5.3, 0.0, 0.0	93.3, 6.7, 0.0, 0.0

[a] Structure determined in the presence of 30 mM Leu.

[b] Abbreviation for the tyrosine analogue, L-4-fluorophenylalanine.

[c] $R_{work} = \sum||F_o| - |F_c||/\sum|F_o|$, where F_o and F_c are the observed and calculated structure factor amplitudes, respectively.

[d] R_{free} is the R-value for r a 5% subset of reflections excluded from refinement.

[e] Number includes protein atoms with alternate conformations.

[f] n/a, not applicable

[g] Average value for the three Trps bound outside of the substrate binding pocket (Trp602, Trp603, and Trp604)

[h] RMSD, root mean square deviation.

[i] Percentage of amino acids in the most favored, allowed, generous, and disallowed regions of the Ramachandran plot, respectively.